Published in final edited form as:

J Pathol. 2017 September ; 243(1): 89–99. doi:10.1002/path.4930.

Conditional abrogation of Transforming Growth Factor Beta Receptor 1 in PTEN-inactivated endometrium promotes endometrial cancer progression in mice

Yang Gao[1], **Pengfei Lin**[1,2], **John P. Lydon**[3], and **Qinglei Li**[1,*]

[1]Department of Veterinary Integrative Biosciences, College of Veterinary Medicine, Texas A&M University, College Station, TX, 77843, USA

[2]Key Laboratory of Animal Biotechnology of the Ministry of Agriculture, College of Veterinary Medicine, Northwest A&F University, Yangling, Shaanxi, 712100, China

[3]Department of Molecular and Cellular Biology, Baylor College of Medicine, Houston, TX, 77030, USA

Abstract

Although a putative role for TGF beta (TGFB) signaling in the pathogenesis of human endometrial cancer has long been proposed, the precise function of TGFB signaling in the development and progression of endometrial cancer remains elusive. Depletion of PTEN in the mouse uterus causes endometrial cancer. To identify the potential role of TGFB signaling in endometrial cancer, we simultaneously deleted TGFB receptor 1 (*Tgfbr1*) and *Pten* in the mouse uterus using Cre-recombinase driven by the progesterone receptor (termed *Pten*$^{d/d}$; *Tgfbr1*$^{d/d}$). We found that *Pten*$^{d/d}$; *Tgfbr1*$^{d/d}$ mice developed severe endometrial lesions that progressed more rapidly compared with those resulting from conditional deletion of *Pten* alone, suggesting that TGFB signaling synergizes with PTEN to suppress endometrial cancer progression. Remarkably, the *Pten*$^{d/d}$; *Tgfbr1*$^{d/d}$ mice developed distant pulmonary metastases, leading to significantly reduced life span. The development of metastasis and accelerated tumor progression in *Pten*$^{d/d}$; *Tgfbr1*$^{d/d}$ mice are associated with increased production of pro-inflammatory chemokines, enhanced cancer cell motility evidenced by myometrial invasion and disruption, and altered tumor microenvironment characterized by recruitment of tumor-associated macrophages. Thus, conditional deletion of *Tgfbr1* in PTEN-inactivated endometrium leads to a disease that recapitulates invasive and lethal human endometrial cancer. This mouse model may be valuable for preclinical testing of new cancer therapies, particularly those targeting metastasis, one of the hallmarks of cancer and a major cause of death in endometrial cancer patients.

*Correspondence to: Qinglei Li, Ph.D., Department of Veterinary Integrative Biosciences, College of Veterinary Medicine & Biomedical Sciences, Texas A&M University, College Station, TX, 77843, USA. Phone: 979 862 2009; Fax: 979 847 8981; qli@cvm.tamu.edu.

Competing Financial Interests: The authors declare no conflict of interest.

Author Contributions Statement: Y.G. and Q. L. designed experiments. Y.G. performed major experiments and P.L. performed some immunostaining. J.P.L. provided *Pgr*-Cre mice. Y.G. and Q.L. wrote the manuscript. All authors approved the manuscript.

Keywords

TGF beta; endometrial cancer; PTEN; TGFBR1; metastasis; mouse model

Introduction

Approximately 61,380 new cases and 10,920 deaths from uterine corpus cancers, the majority of which are endometrial cancers, are projected to occur in 2017 in the United States [1]. There are two major types of endometrial cancer. Type I cancers are mostly endometrioid adenocarcinomas that are associated with excess estrogen. Type II cancers are mainly composed of serous carcinomas which are estrogen independent, with overall poorer prognoses [2]. The mechanisms of endometrial cancer development are not well defined and effective prophylactic and therapeutic approaches are needed. Therefore, understanding the molecular mechanisms underlying the pathogenesis of endometrial cancer is an essential step toward developing novel targeted therapies.

Phosphatase and tensin homolog (*PTEN*), a tumor suppressor gene, is mutated in a variety of human cancers including endometrioid adenocarcinoma. PTEN suppresses the activity of phosphoinositide 3-kinase (PI3K)-AKT signaling pathway by dephosphorylating phosphatidylinositol (3, 4, 5)-trisphosphate (PIP3) that participates in AKT activation. The PI3K-AKT signaling pathway regulates diverse cellular functions, including but not limited to, growth, survival, and metabolism; its abnormal activation is associated with cancer development [3]. Heterozygous *Pten* mice develop neoplasms in multiple organs [4]. Conditional deletion of *Pten* in the mouse uterus using progesterone receptor (*Pgr*)-Cre leads to endometrial cancer formation, supporting a pivotal role of PTEN in endometrial oncogenesis [5].

Cancer cells, particularly those arising from advanced malignancies, can metastasize from the primary site to secondary site(s). Metastasis, consisting of a series of events including local invasion, intravasation, circulation, extravasation, and colonization, is the major cause of morbidity and mortality in cancer patients [6]. To establish distant metastasis, cancer cells originating from the primary site acquire an enhanced ability to migrate and invade. Myometrial invasion is an important factor for the diagnosis and staging of endometrial cancer. The depth of myometrial invasion has been used as a criterion for staging endometrial cancers by the International Federation of Gynecology and Obstetrics (FIGO), where FIGO stages IA and IB refer to endometrial cancers with no or less than half myometrial invasion and those with half or more than half myometrial invasion, respectively [7]. Moreover, a higher risk of extrauterine metastases has been found in endometrial cancer patients with more than 50% myoinvasion compared to those with less than 50% myoinvasion [8]. Endometrial cancer can metastasize to other organs, with the common sites being the lymph nodes, vagina, peritoneum, and lung [9,10]. It has been increasingly recognized that the cancer microenvironment is critical for metastasis by promoting adhesion, survival, extracellular matrix proteolysis, cell migration/invasion, immune escape, and angiogenesis [11]. Chemokines and their receptors are important regulators of many cancer cell properties such as proliferation, invasion, apoptosis, and metastasis [12].

Moreover, tumor-associated macrophages (TAMs), a major population of infiltrating leukocytes and well-known immunosuppressive cells, have been shown to promote cancer growth, invasion, and metastasis [13]. Of note, metastasis has not been reported in the mouse model of endometrial cancer with uterine *Pten* depletion [5,14], indicating a need to create additional models to study the metastatic process and associated mechanisms of this gynecologic malignancy.

Transforming growth factor beta (TGFB) signaling is known to be tumor suppressive. Many essential elements of this pathway including the ligands, receptors, and SMAD transducers are mutated and/or altered in human diseases including cancers [15]. *In vitro* studies suggest that TGFB signaling regulates endometrial cancer cell proliferation, survival, invasion, and metastasis [16-18]. However, the contribution of TGFB signaling to the pathogenesis of endometrial cancer at the organism level remains to be uncovered. Therefore, this study explores the role of TGFB signaling in endometrial cancer development and progression by creating a mouse model that harbors concurrent deletion of *Tgfbr1* and *Pten* in the uterus.

Materials and Methods

Animals

Mice were on a mixed C57BL/6/129 genetic background and the use of mice for this study was approved by the Institutional Animal Care and Use Committee at Texas A&M University. The *Pgr*-Cre and *Tgfbr1*^{flox} mice were generated previously [19,20]. The *Pgr*-Cre mice were obtained from Drs. John Lydon and Francesco DeMayo, and the *Tgfbr1*^{flox} mice were contributed by Dr. Stefan Karlsson and imported from the Matzuk laboratory at Baylor College of Medicine. The *Pten*^{flox} mice were purchased from The Jackson Laboratory (stock # 006440; Bar Harbor, ME, USA) [21]. The genotypes of mice and DNA recombination were analyzed by genomic PCR (supplementary material, Table S1) [20-29].

Histology, immunohistochemistry, and immunofluorescence

Tissue samples were fixed in 10% neutral buffered formalin (Sigma, St. Louis, MO, USA), embedded in paraffin wax, and cut into 5 μm thick sections for hematoxylin and eosin (H&E) staining, immunohistochemistry, or immunofluorescence as described [30]. Antibody details are presented in supplementary material, Table S2.

Western blotting

Western blotting was conducted as described [30] using the indicated primary antibodies (supplementary material, Table S2). Quantification of western blots was performed using NIH ImageJ (version 1.50i). Data are presented as percentage, where the levels of target protein in the *Pten*$^{d/d}$ group were set to 100%.

Enzyme-linked immunosorbent assay (ELISA)

Serum CXCL5 levels were measured using Quantikine ELISA kit (R&D, Minneapolis, MN, USA) according to the manufacturer's instruction. In brief, mouse serum samples were diluted 1:20 and assayed in duplicate, along with CXCL5 controls and working standards. Upon completion of the assay, the optical density (OD) value of each well was measured by

a microplate reader (BioTek, Winooski, VT, USA) at wavelengths of 450 nm and 540 nm. The OD values were corrected by subtracting readings at 540 nm from those at 450 nm. Serum CCL2 concentration was analyzed using a mouse MCP-1/CCL2 ELISA Kit (Sigma) according to the manufacturer's protocol. The concentration of each sample was calculated using an online software (http://elisaanalysis.com).

RNAscope

RNAscope 2.5 HD detection reagent (brown) and mouse *Tgfbr1* probe (catalog No. 406201) were purchased from Advanced Cell Diagnostics (ACD, Newark, CA, USA) and the analysis was performed according to the manufacturer's instructions. In brief, paraffin sections were deparaffinized, pretreated by boiling, and digested using protease before hybridization. Hybridization of the *Tgfbr1* probe set was carried out at 40 °C for 2 h, followed by a series of amplification steps. Brown signals were developed using 3,3′-diaminobenzidine (DAB).

RNA isolation, reverse transcription, and quantitative PCR

Mouse uterine tissues were homogenized in RNA lysis tissue (RLT) buffer (Qiagen, Redwood City, CA, USA). Total RNA was isolated using an RNeasy Mini Kit (Qiagen) based on the manufacturer's protocol, with on-column DNase digestion. The resultant RNA was dissolved in ribonuclease-free water. Reverse transcription was carried out using 200 ng (uterus) or 1 μg (lung) RNA and SuperScript III Reverse Transcriptase (ThermoFisher Scientific, Waltham, MA, USA). Quantitative (real-time) PCR was conducted using a Bio-Rad Real-time PCR Detection System (Hercules, CA, USA). Each assay was performed at least in duplicate using primers listed in supplementary material, Table S1 and iTaq Universal SYBR Green Supermix (Bio-Rad) [29].

Statistical analysis

Statistical analysis was performed using GraphPad Prism (version 7.01). Data are mean ± standard error of the mean (s.e.m.). Comparisons between two means were performed using two-tailed *t*-tests (unpaired). Comparisons of means among multiple groups were performed by one-way analysis of variance (ANOVA) followed by Holm-Sidak pairwise comparisons. Survival curves were analyzed using the Log-rank/Mantel-Cox test. Significantly skewed data were log transformed prior to ANOVA. Statistical significance was defined as $*P < 0.05$, $**P < 0.01$, and $***P < 0.001$.

Results

Generation of mice harboring simultaneous deletion of *Pten* and *Tgfbr1* genes

Pten Pgr-Cre conditional knockout (termed $Pten^{d/d}$) mice develop endometrial cancer [5]. To define the function of TGFB signaling in endometrial cancer, we simultaneously ablated *Pten* and *Tgfbr1* in the mouse uterus using *Pgr*-Cre. To examine the expression of *Tgfbr1* in $Pten^{d/d}$ uteri, we performed RNAscope *in situ* hybridization and demonstrated the localization of *Tgfbr1* mRNA to the hyperplastic uterine epithelia in $Pten^{d/d}$ uteri (supplementary material, Figure S1A, B). Positive and negative controls were depicted (supplementary material, Figure S1C, D). To validate these models, we demonstrated that

Pten and *Tgfbr1* conditional alleles were recombined in the uteri, but not the tails, of *Pten*$^{d/d}$ and/or *Pten*$^{d/d}$; *Tgfbr1*$^{d/d}$ mice (supplementary material, Figure S2A). A significant reduction of mRNA levels of *Pten* and/or *Tgfbr1* was detected in the uteri of *Pten*$^{d/d}$, *Tgfbr1*$^{d/d}$, and *Pten*$^{d/d}$; *Tgfbr1*$^{d/d}$ mice by real-time PCR analysis (supplementary material, Figure S2B-D). Reduction of the protein levels of PTEN in the uteri of *Pten*$^{d/d}$; *Tgfbr1*$^{d/d}$ mice was demonstrated using immunohistochemistry and western blot (supplementary material, Figure S2E-G, K). Consistent with the loss of inhibition of PI3K-AKT pathway, phospho-AKT (pAKT) levels were increased in PTEN-depleted uteri (supplementary material, Figure S2H-K). Thus, we successfully created a mouse model with conditional deletion of *Pten* and *Tgfbr1* in the uterus.

Pten$^{d/d}$; *Tgfbr1*$^{d/d}$ mice develop severe endometrial lesions that progress more rapidly compared to mice with *Pten* deletion alone

Endometrial cancer affects the lifespan of *Pten*$^{d/d}$ mice, beginning around 5 months of age [5]. While all *Pten*$^{d/d}$, *Tgfbr1*$^{d/d}$, *Tgfbr1*$^{f/f}$, *Pten*$^{f/f}$, and *Pten*$^{f/f}$; *Tgfbr1*$^{f/f}$ mice survived past 17 weeks, the *Pten*$^{d/d}$; *Tgfbr1*$^{d/d}$ mice demonstrated significantly shortened lifespan (Figure 1A). Consistent with cancer development, the uterus/body weight ratio was increased in both *Pten*$^{d/d}$ and *Pten*$^{d/d}$; *Tgfbr1*$^{d/d}$ mice versus *Tgfbr1*$^{f/f}$, *Pten*$^{f/f}$, *Pten*$^{f/f}$; *Tgfbr1*$^{f/f}$, and *Tgfbr1*$^{d/d}$ mice at both 4 and 9 weeks of age (supplementary material, Figure S3A, B). The uterine cancer in *Pten*$^{d/d}$; *Tgfbr1*$^{d/d}$ mice was generally more hemorrhagic and/or locally invasive (Figure 1B). *Tgfbr1*$^{d/d}$ mice did not develop endometrial cancer despite the observation of cystic endometrial glands and adenomyosis in 8-month-old mice (data not shown). Thus, this mouse line was not the focus of subsequent studies.

To determine potential phenotypic differences in endometrial cancer development between *Pten*$^{d/d}$ and *Pten*$^{d/d}$; *Tgfbr1*$^{d/d}$ mice, we performed H&E staining and immunohistochemical analyses of E-cadherin (ECAD), an epithelial marker, using uteri from *Pten*$^{d/d}$, *Pten*$^{d/d}$; *Tgfbr1*$^{d/d}$, and corresponding control mice at various stages. Atypical endometrial hyperplasia was found at the age of 10 days (not shown) and 2 weeks in both *Pten*$^{d/d}$ and *Pten*$^{d/d}$; *Tgfbr1*$^{d/d}$ mice (supplementary material, Figure S4A-F). Dramatic differences between *Pten*$^{d/d}$; *Tgfbr1*$^{d/d}$ and *Pten*$^{d/d}$ mice were not found at 2 weeks of age, except the presence of more hyperplastic epithelia in some *Pten*$^{d/d}$; *Tgfbr1*$^{d/d}$ mice (Figure 2A-D; supplementary material, Figure S4A-F). At the age of 4 weeks, the atypical endometrial hyperplasia in *Pten*$^{d/d}$ mice progressed to carcinoma. In contrast, *Pten*$^{d/d}$; *Tgfbr1*$^{d/d}$ mice developed more severe lesions with the presence of large foci of adenocarcinoma accompanied by degenerating cells within the central region in some mice (Figure 2E-H; supplementary material, Figure S4G-L). Of note, endometrial cancers in both *Pten*$^{d/d}$ and *Pten*$^{d/d}$; *Tgfbr1*$^{d/d}$ mice were positive for estrogen receptor (ER) and PGR at this stage (supplementary material, Figure S5A-H). However, a reduction of PGR but not ER signals was observed in *Pten*$^{d/d}$; *Tgfbr1*$^{d/d}$ mice at a later stage (Figure 2I-P; supplementary material, Figure S5I). At the age of 2 months, although myoinvasion could be observed in both *Pten*$^{d/d}$ and *Pten*$^{d/d}$; *Tgfbr1*$^{d/d}$ mice (supplementary material, Figure S6A-D), *Pten*$^{d/d}$; *Tgfbr1*$^{d/d}$ uteri demonstrated a haphazard glandular pattern, desmoplastic stroma, and more severe myometrial disruption (supplementary material, Figure S6E, F; Figure 3A-E). Immunohistochemical analysis using a smooth muscle marker, calponin 1 (CNN1), revealed

that *Pten*$^{d/d}$ mice had recognizable myometrial layers at 2 months of age (Figure 3A, B, E), while severely disrupted myometrial layers intermingled with epithelial cancer cells were found in approximately 69% of *Pten*$^{d/d}$; *Tgfbr1*$^{d/d}$ mice (Figure 3C, D, E). No myometrial abnormality was found in *Tgfbr1*$^{d/d}$ and *Tgfbr1*$^{f/f}$ mice at the examined time stage (data not shown). To better visualize epithelial and myometrial compartments, we performed double immunofluorescence using anti-cytokeratin 8 (KRT8) and CNN1 antibodies to label the respective epithelium and smooth muscle (Figure 3F-M). The results revealed that cancer epithelia breached the uterine wall in *Pten*$^{d/d}$; *Tgfbr1*$^{d/d}$ mice (Figure 3J-M) versus *Pten*$^{d/d}$ mice (Figure 3F-I). Thus, these results provide *in vivo* evidence of accelerated endometrial cancer progression and enhanced cell invasion in mice with conditional deletion of *Pten* and *Tgfbr1*.

Pten$^{d/d}$; *Tgfbr1*$^{d/d}$ mice develop pulmonary metastasis

Metastasis is a major cause of death in endometrial cancer patients [9,10]. In contrast to the *Pten*$^{d/d}$ mice where visible metastasis in distant organs was not observed even at 25-36 weeks of age (supplementary material, Table S3), *Pten*$^{d/d}$; *Tgfbr1*$^{d/d}$ mice developed distant organ metastasis, preferentially in the lung. At the advanced stage of disease development (i.e., 7-16 weeks), no grossly visible metastases were observed in the bladder, heart, kidney, and spleen (supplementary material, Table S3), although microscopically detectable metastases positive for KRT8 and ER could be found in the lymph nodes of *Pten*$^{d/d}$; *Tgfbr1*$^{d/d}$ and *Pten*$^{d/d}$ mice (supplementary material, Figure S7). In contrast, grossly visible metastases were evident in the lungs of *Pten*$^{d/d}$; *Tgfbr1*$^{d/d}$ mice (Figure 4A; supplementary material, Figure S8A, Table S3). Unlike the lungs of *Pten*$^{d/d}$ mice comprising highly organized alveoli structures (Figure 4B), the lungs of *Pten*$^{d/d}$; *Tgfbr1*$^{d/d}$ mice demonstrated multiple metastatic sites, consisting of pathological lesions with variable differentiation status (Figure 4C-G). In addition, the metastasis was frequently accompanied by hemorrhage and loss of morphologically normal alveoli (supplementary material, Figure S8A; Figure 4C-G). Using immunohistochemistry, we further verified that the metastatic nodules were positive for KRT8 (Figure 4I; supplementary material, Figure S8C) and ER (Figure 4K), but were negative for PGR (Figure 4M). Of note, analysis of ER expression in the lungs of *Pten*$^{d/d}$; *Tgfbr1*$^{d/d}$ mice demonstrated the formation of endometrial gland-like lesions within the metastatic nodules (supplementary material, Figure S8D, E). Furthermore, recombined *Tgfbr1/Pten* conditional alleles were detected in the lung metastases of Pten$^{d/d}$; *Tgfbr1*$^{d/d}$ mice but not in the lung tissues of Pten$^{d/d}$ mice (supplementary material, Figure S8F). The metastatic nodules also expressed mucin 1 (MUC1; Figure 4O), a protein that is frequently overexpressed in metastatic cancers [31]. Immunostaining of the lungs from *Pten*$^{f/f}$; *Tgfbr1*$^{f/f}$ controls were representatively shown (Figure 4H, J, L, N). To confirm that pulmonary metastasis was specific to *Pten*$^{d/d}$; *Tgfbr1*$^{d/d}$ mice, we analyzed age-matched lungs from *Pten*$^{d/d}$ and *Pten*$^{f/f}$ mice and did not find metastasis in these mice (data not shown).

Loss of TGFBR1 increases the production of pro-inflammatory chemokines associated with cancer metastasis

Chemoattractant cytokines, or chemokines, and their receptors play important roles in many carcinogenic events [32]. To determine the potential mechanism of metastasis resulting from

ablation of TGFBR1, we compared uterine mRNA expression of chemokines including C-X-C motif ligand 1 (*Cxcl1*), *Cxcl5*, *Cxcl12*, chemokine (C-C motif) ligand 2 (*Ccl2*), and *Ccl9* and a chemokine receptor *Cxcr2* that are involved in metastasis [33-36] between *Pten*$^{d/d}$; *Tgfbr1*$^{d/d}$ and *Pten*$^{d/d}$ mice, along with *Pten*$^{f/f}$; *Tgfbr1*$^{f/f}$ and *Pten*$^{f/f}$ controls. Results showed that the transcript levels of *Cxcl5* and its receptor *Cxcr2* were increased in the uteri of *Pten*$^{d/d}$; *Tgfbr1*$^{d/d}$ mice versus *Pten*$^{d/d}$ and control mice at 2 weeks of age (Figure 5B, D), while those of *Cxcl1* (Figure 5A), *Cxcl12* (Figure 5C), *Ccl2* (Figure 5E), and *Ccl9* (Figure 5F) were comparable between *Pten*$^{d/d}$; *Tgfbr1*$^{d/d}$ and *Pten*$^{d/d}$ mice at this timepoint. To determine whether there was a correlation between serum CXCL5 levels and cancer progression and metastasis, we performed ELISA and demonstrated significantly elevated serum CXCL5 levels in *Pten*$^{d/d}$; *Tgfbr1*$^{d/d}$ mice versus *Pten*$^{d/d}$ and control mice at 9 weeks of age (Figure 5G). Interestingly, serum CCL2 levels were also increased in 9-week-old *Pten*$^{d/d}$; *Tgfbr1*$^{d/d}$ mice (Figure 5H). Further analysis revealed significantly upregulated mRNA levels of *Ccl2* and *Cxcl5* in the lung metastases of 9-week-old *Pten*$^{d/d}$; *Tgfbr1*$^{d/d}$ mice versus age-matched *Pten*$^{d/d}$ mice (Figure 5I), suggesting the lung metastases may serve as a potential source of the elevated serum levels of these chemokines. Furthermore, CXCL5 was localized to the metastatic nodules within the lungs of *Pten*$^{d/d}$; *Tgfbr1*$^{d/d}$ mice versus *Pten*$^{d/d}$ mice (Figure 5J, K). These results suggest a potential involvement of CXCL5/CCL2 in endometrial cancer progression in *Pten*$^{d/d}$; *Tgfbr1*$^{d/d}$ mice.

Recruitment of tumor-associated macrophages in *Pten*$^{d/d}$; *Tgfbr1*$^{d/d}$ uteri

TGFB signaling regulates CXCL5 secretion in mammary cancer cells and recruits immune cells including TAMs to promote tumor progression [34,35]. TAMs can acquire a polarized M2 phenotype (i.e., M2 macrophage or alternatively activated macrophage) and promote tumor progression [37]. We therefore examined the potential involvement of TAMs in tumor progression in *Pten*$^{d/d}$; *Tgfbr1*$^{d/d}$ mice by immunohistochemistry using antibodies directed to CD163 (a marker for M2 macrophages) [38]. F4/80, a well-established marker of murine macrophages [39], was used to monitor the macrophage population in the uteri. The presence of F4/80^{+} macrophages was revealed in the stroma of both *Pten*$^{d/d}$ and *Pten*$^{d/d}$; *Tgfbr1*$^{d/d}$ tumors at 9 weeks of age (Figure 6A, C). Interestingly, cells positive for CD163 were readily detectable in the uteri of *Pten*$^{d/d}$; *Tgfbr1*$^{d/d}$ mice *versus Pten*$^{d/d}$ mice (Figure 6B, D). Positive and negative controls were included (Figure 6E, F). Consistent with the immunohistochemical observation, western blotting showed that CD163 expression was significantly increased in *Pten*$^{d/d}$; *Tgfbr1*$^{d/d}$ mice compared with *Pten*$^{d/d}$ mice (Figure 6G, H). Immunostaining of F4/80 and CD163 using age-matched *Pten*$^{f/f}$ and *Pten*$^{f/f}$; *Tgfbr1*$^{f/f}$ mice was included in supplementary material, Figure S9. These findings suggest a potential role of TAMs in endometrial cancer progression in *Pten*$^{d/d}$; *Tgfbr1*$^{d/d}$ mice.

Discussion

Mutation or inactivation of TGFB signaling components has been associated with the development of a broad array of cancers [40]. Although a putative role for TGFB signaling in the pathogenesis of human endometrial cancer has long been proposed [41], the precise function of TGFB signaling in endometrial cancer development has remained elusive. *PTEN* mutations have been identified in a variety of cancers. Loss of PTEN, a negative regulator of

the PI3K-AKT pathway, is involved in the oncogenesis of endometrial carcinoma [42]. Conditional deletion of *Pten* in the mouse uterus using *Pgr*-Cre leads to the development of endometrial malignancy, which phenocopies many pathological characteristics of the human endometrial cancer [5]. As a result, the *Pten*$^{d/d}$ mouse model has been used to study endometrial cancer development [14,43,44]. However, *Pten*$^{d/d}$ mice do not develop visible organ metastasis, a cause of recurrence after surgical intervention for primary cancers. Recurrence of endometrial cancer resulting from either local or distant metastases remains devastating. Endometrial cancer has been reported to have the highest frequency of pulmonary metastases (20-25%) *versus* other gynecologic cancers [9,10]. Therefore, development of an endometrial cancer model with organ metastases mimicking human endometrial cancer is critical to understand metastatic initiation and progression.

Little is known about the potential interplay between TGFB signaling and PTEN during endometrial carcinogenesis although their interactions have been documented in other tumors [45,46]. Inactivation of TGFB signaling and loss of growth inhibition are associated with the development of human endometrial cancer [47,48]. It has been shown that mutations of TGFB signaling components including TGFB receptors and SMADs and alteration of TGFB signaling activity reflected by changes in gene expression and/or phosphorylation of key signaling proteins play a role in the pathoetiology of human endometrial cancer [47,49,50]. TGFBR1 has a 5.6% mutation and alteration rate in human endometrial cancer [49,51]. As reported, cancerous human endometrium expresses lower levels of TGFBR1 protein [47,52]. TGFBR2 is mutated/altered in 6.5% endometrial tumors [49,51]. Studies from The Cancer Genome Atlas (TCGA) Research Network have also suggested alterations of several SMADs in human endometrial cancer [49,51]. Of particular importance was the availability of the two endometrial cancer models (i.e., *Pten*$^{d/d}$ and *Pten*$^{d/d}$; *Tgfbr1*$^{d/d}$ mice) that demonstrated distinct pulmonary metastatic outcomes depending on the status of a known TGFB signaling component (i.e., TGFBR1) in the PTEN-inactivated uterus. Therefore, the aforementioned mutations and/or dysregulation of TGFB signaling components in endometrial cancer and the development of pulmonary metastasis in *Pten*$^{d/d}$; *Tgfbr1*$^{d/d}$ mice make this model a valuable tool to study the pathogenesis and progression of endometrioid adenocarcinoma, the most frequent type of endometrial cancer in women. However, it needs to be pointed out that due to the expression of *Pgr*-Cre in uterine stromal cells and the myometrium, a potential impact of TGFBR1 and/or PTEN loss in these cellular compartments on the tumor phenotype cannot be excluded, which may represent a limitation of the current study. Future investigations are needed to address this question using Cre lines targeting distinct cellular compartments of the uterus.

Metastasis is a complex process where cancer cells can disseminate via the bloodstream and/or lymphatics to establish secondary tumors at the metastatic sites. Because of the invlovment of chemokines in the process of metastasis, therapeutic strategies targeting the action of chemokines may block/attenuate metastasis. A functional link between TGFB signaling and chemokines during cancer metastasis has emerged [33,53,54]. In one study, conditional ablation of TGFBR2 in mammary fibroblasts increased the secretion of CCL2, which promoted mammary cancer progression at least partially through a TAM-dependent mechanism [33]. Enhanced production of CCL9 resulting from loss of TGFB signaling

promotes immature myeloid cell infiltration and the development of invasive intestinal tumors [55]. Loss of TGFB signaling in mouse mammary epithelial cells promotes metastasis by recruiting myeloid-derived suppressor cells into tumor tissues via CXCL5-CXCR2 and CXCL12-CXCR4 axes [34]. The increased transcript levels of *Cxcl5* and its receptor *Cxcr2* in the uteri of *Pten*$^{d/d}$; *Tgfbr1*$^{d/d}$ mice suggest a potential common mechanism of CXCL5/CCL2 upregulation in the absence of TGFB receptor-mediated signaling in epithelial cancer cells [34]. This finding together with the role of CXCL5 in cell invasion and metastasis in several types of cancers including bladder cancer [56], mammary cancer [34], and liver cancer [57] suggest that activation of the CXCL5-CXCR2 axis due to loss of TGFBR1 may contribute to the pulmonary metastasis of endometrial cancer induced by conditional abrogation of PTEN in the uterus. Importantly, we showed that serum levels of CXCL5 and CCL2 were elevated in *Pten*$^{d/d}$; *Tgfbr1*$^{d/d}$ mice compared with *Pten*$^{d/d}$ mice. Since *CXCL5* expression is increased in human endometrial cancer tissues compared with normal endometrium [58], it is plausible to further explore the potential of CXCL5 and CCL2 as biomarkers for endometrial cancer patients.

Studies using genetically modified mice have revealed the emerging role of TAMs in the development of invasive endometrial cancer [59,60]. However, the involvement of uterine TGFB signaling in TAM recruitment and polarization and the contribution of TAMs to the development of endometrial cancer remain to be elucidated. At advanced stages of tumor development, CD163^{+} cells were readily detectable and the expression of CD163 was increased in the uteri of *Pten*$^{d/d}$; *Tgfbr1*$^{d/d}$ mice versus *Pten*$^{d/d}$ mice, suggesting the involvement of TAMs in promoting endometrial cancer progression in *Pten*$^{d/d}$; *Tgfbr1*$^{d/d}$ mice. Future studies are warranted to define the mechanism of action of pro-inflammatory chemokines, particularly CXCL5 and CCL2, and the function of TAMs within the tumor microenvironment in our model. It is noteworthy that TGFB signaling may act as a tumor suppressor in pre-malignant cells but as a tumor promoter during advanced tumor development [61]. That the deletion of *Tgfbr1* in PTEN-inactivated uterus accelerates endometrial cancer progression also highlights the complex role of TGFB signaling *in vivo*, where compensatory pathways may function to promote cancer invasion/metastasis in the absence of TGFBR1.

In summary, conditional deletion of *Pten* and *Tgfbr1* leads to a disease that recapitulates invasive and lethal endometrial cancer. This new mouse model is potentially valuable for preclinical testing of targeted therapies to treat endometrial cancer with metastasis.

Supplementary Material

Refer to Web version on PubMed Central for supplementary material.

Acknowledgments

We thank Dr. Kayla Bayless for critical reading of the manuscript and Dr. Robert Burghardt for helpful discussions. The authors also wish to thank Dr. Francesco DeMayo for the help with importing *Pgr*-Cre mice, Ms. Yating Cheng for suggestions on ELISA analysis, and Ms. Xin Fang and Nan Ni for technical assistance. This research is supported in part by the New Faculty Start-up Funds from Texas A&M University and the National Institutes of Health grant R21HD073756 from the Eunice Kennedy Shriver National Institute of Child Health & Human Development (to Q.L.).

References

1. Siegel RL, Miller KD, Jemal A. Cancer Statistics, 2017. CA Cancer J Clin. 2017; 67:7–30. [PubMed: 28055103]
2. Setiawan VW, Yang HP, Pike MC, et al. Type I and II endometrial cancers: Have they different risk factors? J Clin Oncol. 2013; 31:2607–2618. [PubMed: 23733771]
3. Engelman JA. Targeting PI3K signalling in cancer: opportunities, challenges and limitations. Nat Rev Cancer. 2009; 9:550–562. [PubMed: 19629070]
4. Podsypanina K, Ellenson LH, Nemes A, et al. Mutation of Pten/Mmac1 in mice causes neoplasia in multiple organ systems. Proc Natl Acad Sci U S A. 1999; 96:1563–1568. [PubMed: 9990064]
5. Daikoku T, Hirota Y, Tranguch S, et al. Conditional loss of uterine Pten unfailingly and rapidly induces endometrial cancer in mice. Cancer Res. 2008; 68:5619–5627. [PubMed: 18632614]
6. Nguyen DX, Bos PD, Massague J. Metastasis: from dissemination to organ-specific colonization. Nat Rev Cancer. 2009; 9:274–284. [PubMed: 19308067]
7. Pecorelli S. Revised FIGO staging for carcinoma of the vulva, cervix, and endometrium. Int J Gynaecol Obstet. 2009; 105:103–104. [PubMed: 19367689]
8. Larson DM, Connor GP, Broste SK, et al. Prognostic significance of gross myometrial invasion with endometrial cancer. Obstet Gynecol. 1996; 88:394–398. [PubMed: 8752246]
9. Sohaib SA, Houghton SL, Meroni R, et al. Recurrent endometrial cancer: patterns of recurrent disease and assessment of prognosis. Clin Radiol. 2007; 62:28–34. [PubMed: 17145260]
10. Kurra V, Krajewski KM, Jagannathan J, et al. Typical and atypical metastatic sites of recurrent endometrial carcinoma. Cancer Imaging. 2013; 13:113–122. [PubMed: 23545091]
11. Bogenrieder T, Herlyn M. Axis of evil: molecular mechanisms of cancer metastasis. Oncogene. 2003; 22:6524–6536. [PubMed: 14528277]
12. Sarvaiya PJ, Guo D, Ulasov I, et al. Chemokines in tumor progression and metastasis. Oncotarget. 2013; 4:2171–2185. [PubMed: 24259307]
13. Galdiero MR, Bonavita E, Barajon I, et al. Tumor associated macrophages and neutrophils in cancer. Immunobiology. 2013; 218:1402–1410. [PubMed: 23891329]
14. Lindberg ME, Stodden GR, King ML, et al. Loss of CDH1 and Pten accelerates cellular invasiveness and angiogenesis in the mouse uterus. Biol Reprod. 2013; 89:8. [PubMed: 23740945]
15. Gordon KJ, Blobe GC. Role of transforming growth factor-β superfamily signaling pathways in human disease. Biochim Biophys Acta. 2008; 1782:197–228. [PubMed: 18313409]
16. Anzai Y, Gong Y, Holinka CF, et al. Effects of transforming growth factors and regulation of their mRNA levels in two human endometrial adenocarcinoma cell lines. J Steroid Biochem Mol Biol. 1992; 42:449–455. [PubMed: 1616874]
17. Van Themsche C, Mathieu I, Parent S, et al. Transforming growth factor-beta3 increases the invasiveness of endometrial carcinoma cells through phosphatidylinositol 3-kinase-dependent up-regulation of X-linked inhibitor of apoptosis and protein kinase c-dependent induction of matrix metalloproteinase-9. J Biol Chem. 2007; 282:4794–4802. [PubMed: 17150964]
18. Lei X, Wang L, Yang J, et al. TGFbeta signaling supports survival and metastasis of endometrial cancer cells. Cancer Manag Res. 2009; 2009:15–24. [PubMed: 20622970]
19. Soyal SM, Mukherjee A, Lee KY, et al. Cre-mediated recombination in cell lineages that express the progesterone receptor. Genesis. 2005; 41:58–66. [PubMed: 15682389]
20. Larsson J, Goumans MJ, Sjostrand LJ, et al. Abnormal angiogenesis but intact hematopoietic potential in TGF-beta type I receptor-deficient mice. Embo J. 2001; 20:1663–1673. [PubMed: 11285230]
21. Lesche R, Groszer M, Gao J, et al. Cre/loxP-mediated inactivation of the murine Pten tumor suppressor gene. Genesis. 2002; 32:148–149. [PubMed: 11857804]
22. Li Q, Agno JE, Edson MA, et al. Transforming growth factor beta receptor type 1 is essential for female reproductive tract integrity and function. PLoS Genet. 2011; 7:e1002320. [PubMed: 22028666]
23. Nagashima T, Li Q, Clementi C, et al. BMPR2 is required for postimplantation uterine function and pregnancy maintenance. J Clin Invest. 2013; 123:2539–2550. [PubMed: 23676498]

24. Park SO, Lee YJ, Seki T, et al. ALK5- and TGFBR2-independent role of ALK1 in the pathogenesis of hereditary hemorrhagic telangiectasia type 2. Blood. 2008; 111:633–642. [PubMed: 17911384]
25. Zeng N, Yang KT, Bayan JA, et al. PTEN controls beta-cell regeneration in aged mice by regulating cell cycle inhibitor p16ink4a. Aging Cell. 2013; 12:1000–1011. [PubMed: 23826727]
26. Li L, Huang LP, Vergis AL, et al. IL-17 produced by neutrophils regulates IFN-gamma-mediated neutrophil migration in mouse kidney ischemia-reperfusion injury. J Clin Invest. 2010; 120:331–342. [PubMed: 20038794]
27. Duchene J, Lecomte F, Ahmed S, et al. A novel inflammatory pathway involved in leukocyte recruitment: role for the kinin B1 receptor and the chemokine CXCL5. J Immunol. 2007; 179:4849–4856. [PubMed: 17878384]
28. Saur D, Seidler B, Schneider G, et al. CXCR4 expression increases liver and lung metastasis in a mouse model of pancreatic cancer. Gastroenterology. 2005; 129:1237–1250. [PubMed: 16230077]
29. Gao Y, Bayless KJ, Li Q. TGFBR1 is required for mouse myometrial development. Mol Endocrinol. 2014; 28:380–394. [PubMed: 24506537]
30. Gao Y, Vincent DF, Davis AJ, et al. Constitutively active transforming growth factor beta receptor 1 in the mouse ovary promotes tumorigenesis. Oncotarget. 2016; 7:40904–40918. [PubMed: 27344183]
31. Horm TM, Schroeder JA. MUC1 and metastatic cancer: expression, function and therapeutic targeting. Cell Adh Migr. 2013; 7:187–198. [PubMed: 23303343]
32. Lazennec G, Richmond A. Chemokines and chemokine receptors: new insights into cancer-related inflammation. Trends Mol Med. 2010; 16:133–144. [PubMed: 20163989]
33. Hembruff SL, Jokar I, Yang L, et al. Loss of transforming growth factor-beta signaling in mammary fibroblasts enhances CCL2 secretion to promote mammary tumor progression through macrophage-dependent and -independent mechanisms. Neoplasia. 2010; 12:425–433. [PubMed: 20454514]
34. Yang L, Huang J, Ren X, et al. Abrogation of TGF beta signaling in mammary carcinomas recruits Gr-1+CD11b+ myeloid cells that promote metastasis. Cancer Cell. 2008; 13:23–35. [PubMed: 18167337]
35. Novitskiy SV, Pickup MW, Gorska AE, et al. TGF-beta receptor II loss promotes mammary carcinoma progression by Th17 dependent mechanisms. Cancer Discov. 2011; 1:430–441. [PubMed: 22408746]
36. Yan HH, Jiang J, Pang Y, et al. CCL9 induced by TGFbeta signaling in myeloid cells enhances tumor cell survival in the premetastatic organ. Cancer Res. 2015; 75:5283–5298. [PubMed: 26483204]
37. Sica A, Invernizzi P, Mantovani A. Macrophage plasticity and polarization in liver homeostasis and pathology. Hepatology. 2014; 59:2034–2042. [PubMed: 24115204]
38. Komohara Y, Niino D, Saito Y, et al. Clinical significance of CD163(+) tumor-associated macrophages in patients with adult T-cell leukemia/lymphoma. Cancer Sci. 2013; 104:945–951. [PubMed: 23557330]
39. Austyn JM, Gordon S. F4/80, a monoclonal-antibody directed specifically against the mouse macrophage. Eur J Immunol. 1981; 11:805–815. [PubMed: 7308288]
40. de Caestecker MP, Piek E, Roberts AB. Role of transforming growth factor-beta signaling in cancer. J Natl Cancer Inst. 2000; 92:1388–1402. [PubMed: 10974075]
41. Gold LI, Parekh TV. Loss of growth regulation by transforming growth factor-beta (TGF-beta) in human cancers: Studies on endometrial carcinoma. Semin Reprod Endocrinol. 1999; 17:73–92. [PubMed: 10406078]
42. Tashiro H, Blazes MS, Wu R, et al. Mutations in PTEN are frequent in endometrial carcinoma but rare in other common gynecological malignancies. Cancer Res. 1997; 57:3935–3940. [PubMed: 9307275]
43. Kim TH, Yoo JY, Kim HI, et al. Mig-6 suppresses endometrial cancer associated with Pten deficiency and ERK activation. Cancer Res. 2014; 74:7371–7382. [PubMed: 25377472]

44. Kim TH, Franco HL, Jung SY, et al. The synergistic effect of Mig-6 and Pten ablation on endometrial cancer development and progression. Oncogene. 2010; 29:3770–3780. [PubMed: 20418913]
45. Xu X, Ehdaie B, Ohara N, et al. Synergistic action of Smad4 and Pten in suppressing pancreatic ductal adenocarcinoma formation in mice. Oncogene. 2010; 29:674–686. [PubMed: 19901970]
46. Bian Y, Hall B, Sun ZJ, et al. Loss of TGF-beta signaling and PTEN promotes head and neck squamous cell carcinoma through cellular senescence evasion and cancer-related inflammation. Oncogene. 2012; 31:3322–3332. [PubMed: 22037217]
47. Parekh TV, Gama P, Wen X, et al. Transforming growth factor beta signaling is disabled early in human endometrial carcinogenesis concomitant with loss of growth inhibition. Cancer Res. 2002; 62:2778–2790. [PubMed: 12019154]
48. Lecanda J, Parekh TV, Gama P, et al. Transforming growth factor-beta, estrogen, and progesterone converge on the regulation of p27Kip1 in the normal and malignant endometrium. Cancer Res. 2007; 67:1007–1018. [PubMed: 17283133]
49. Eritja, N., Yeramian, A., Chen, BJ., et al. Endometrial Carcinoma: Specific Targeted Pathways. In: Ellenson, LH., editor. Molecular Genetics of Endometrial Carcinoma. Springer International Publishing; Cham: 2017. p. 149-207.
50. Piestrzeniewicz-Ulanska, D., McGuinness, DH., Yeaman, GR. TGF-β Signaling in Endometrial Cancer. In: Volume II: Cancer Treatment and Therapy. Jakowlew, SB., editor. Transforming Growth Factor-β in Cancer Therapy. Humana Press; Totowa: 2008. p. 63-78.
51. Kandoth C, Schultz N, Cherniack AD, et al. Integrated genomic characterization of endometrial carcinoma. Nature. 2013; 497:67–73. [PubMed: 23636398]
52. Piestrzeniewicz-Ulanska D, Brys M, Semczuk A, et al. Expression of TGF-beta type I and II receptors in normal and cancerous human endometrium. Cancer Lett. 2002; 186:231–239. [PubMed: 12213293]
53. Bierie B, Chung CH, Parker JS, et al. Abrogation of TGF-beta signaling enhances chemokine production and correlates with prognosis in human breast cancer. J Clin Invest. 2009; 119:1571–1582. [PubMed: 19451693]
54. Itatani Y, Kawada K, Fujishita T, et al. Loss of SMAD4 from colorectal cancer cells promotes CCL15 expression to recruit CCR1+ myeloid cells and facilitate liver metastasis. Gastroenterology. 2013; 145:1064–1075. [PubMed: 23891973]
55. Kitamura T, Kometani K, Hashida H, et al. SMAD4-deficient intestinal tumors recruit CCR1+ myeloid cells that promote invasion. Nat Genet. 2007; 39:467–475. [PubMed: 17369830]
56. Gao Y, Guan Z, Chen J, et al. CXCL5/CXCR2 axis promotes bladder cancer cell migration and invasion by activating PI3K/AKT-induced upregulation of MMP2/MMP9. Int J Oncol. 2015; 47:690–700. [PubMed: 26058729]
57. Zhou SL, Dai Z, Zhou ZJ, et al. Overexpression of CXCL5 mediates neutrophil infiltration and indicates poor prognosis for hepatocellular carcinoma. Hepatology. 2012; 56:2242–2254. [PubMed: 22711685]
58. Wong YF, Cheung TH, Lo KW, et al. Identification of molecular markers and signaling pathway in endometrial cancer in Hong Kong Chinese women by genome-wide gene expression profiling. Oncogene. 2007; 26:1971–1982. [PubMed: 17043662]
59. Pena CG, Nakada Y, Saatcioglu HD, et al. LKB1 loss promotes endometrial cancer progression via CCL2-dependent macrophage recruitment. J Clin Invest. 2015; 125:4063–4076. [PubMed: 26413869]
60. Stodden GR, Lindberg ME, King ML, et al. Loss of Cdh1 and Trp53 in the uterus induces chronic inflammation with modification of tumor microenvironment. Oncogene. 2015; 34:2471–2482. [PubMed: 24998851]
61. Massague J. TGFbeta signalling in context. Nat Rev Mol Cell Biol. 2012; 13:616–630. [PubMed: 22992590]

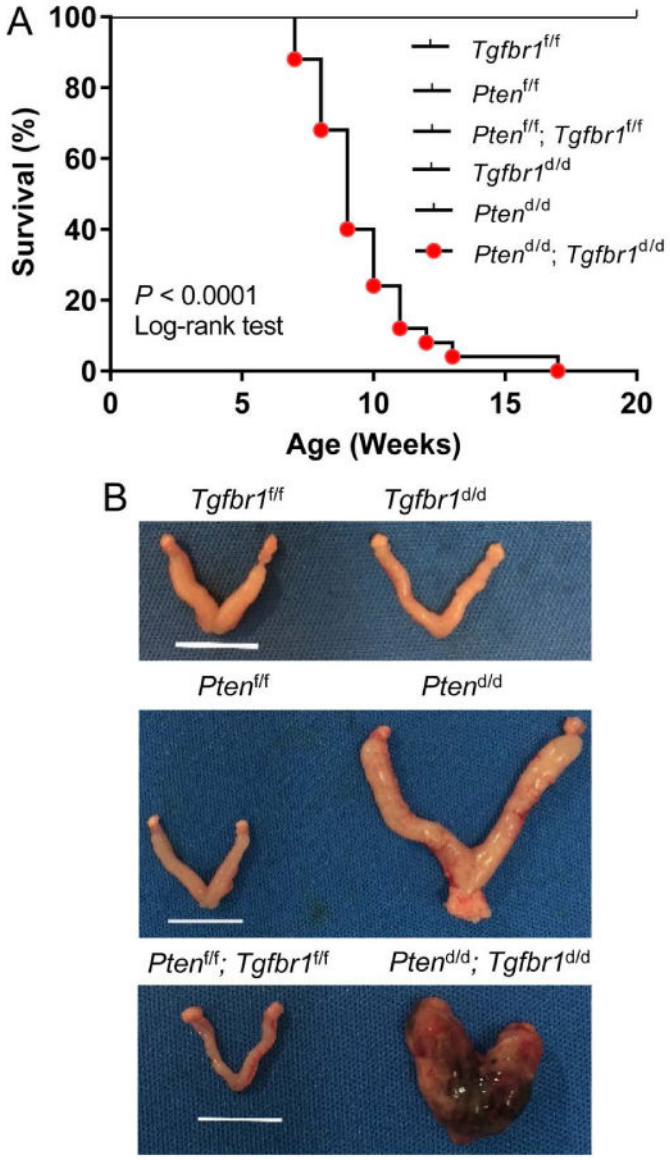

Figure 1.

Simultaneous deletion of *Pten* and *Tgfbr1* in the uterus leads to severe endometrial lesions at an early age. (A) Survival rate of *Tgfbr1*$^{f/f}$ (n = 14), *Pten*$^{f/f}$ (n = 12), *Pten*$^{f/f}$; *Tgfbr1*$^{f/f}$ (n = 10), *Tgfbr1*$^{d/d}$ (n = 19), *Pten*$^{d/d}$ (n = 13), and *Pten*$^{d/d}$; *Tgfbr1*$^{d/d}$ (n = 25) mice. Note the reduced lifespan of *Pten*$^{d/d}$; *Tgfbr1*$^{d/d}$ mice compared with *Tgfbr1*$^{f/f}$, *Pten*$^{f/f}$, *Pten*$^{f/f}$; *Tgfbr1*$^{f/f}$, *Tgfbr1*$^{d/d}$, and *Pten*$^{d/d}$ mice. $P < 0.0001$ (Log-rank/Mantel-Cox test). (B) Macroscopic analysis of uterine cancer from 8-week-old *Pten*$^{d/d}$ and *Pten*$^{d/d}$; *Tgfbr1*$^{d/d}$ mice. Note that the uterine cancer from *Pten*$^{d/d}$; *Tgfbr1*$^{d/d}$ mice was hemorrhagic and locally invasive compared with that from *Pten*$^{d/d}$ mice. *Tgfbr1*$^{f/f}$, *Tgfbr1*$^{d/d}$, *Pten*$^{f/f}$, and *Pten*$^{f/f}$; *Tgfbr1*$^{f/f}$ uteri were morphologically normal. Scale bar = 10 mm.

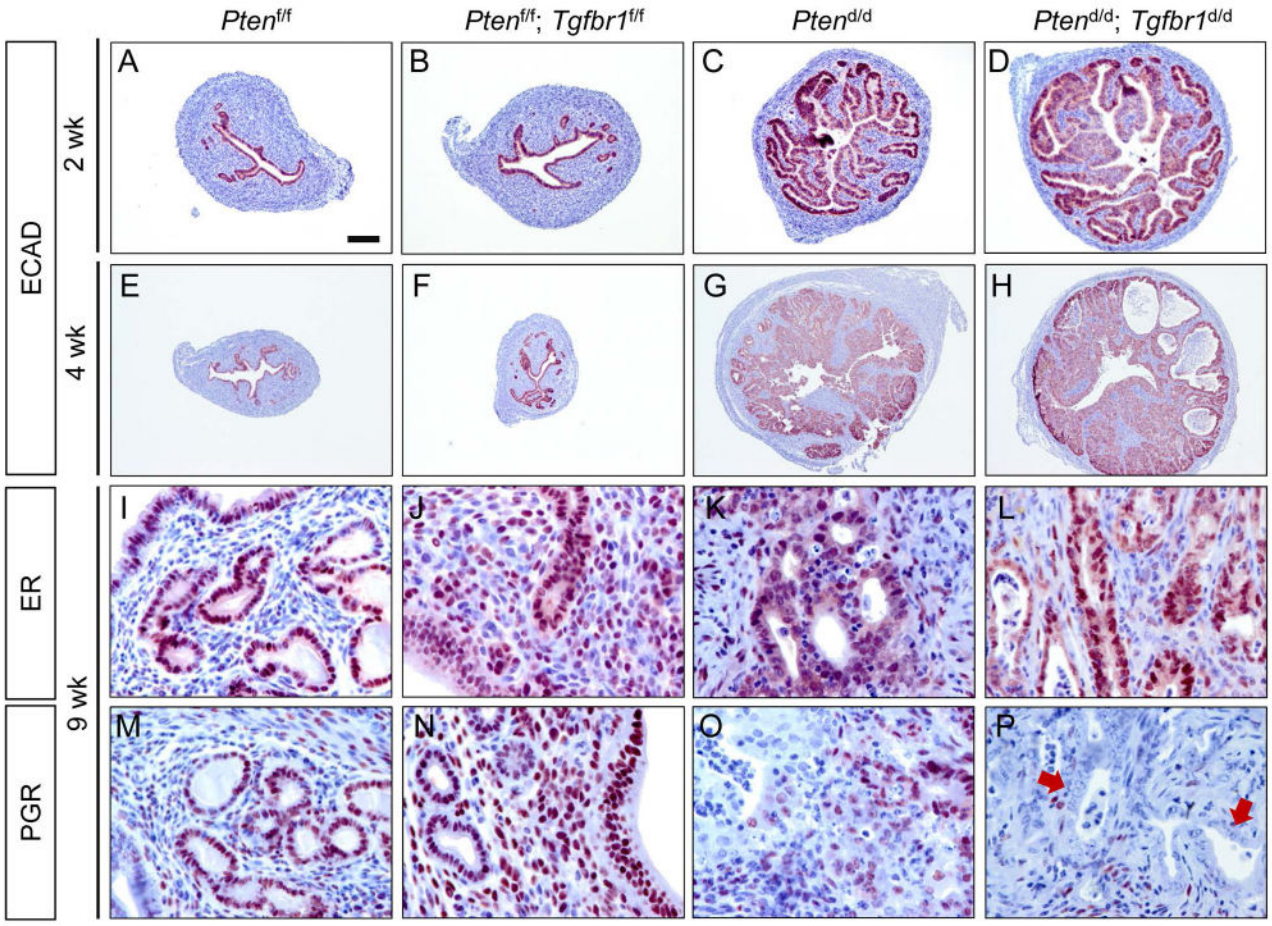

Figure 2.

Enhanced tumor progression in mice with uterine ablation of *TGFBR1* and *PTEN*. (A-H) Immunostaining of ECAD in the uteri of *Pten*$^{f/f}$, *Pten*$^{f/f}$; *Tgfbr1*$^{f/f}$, *Pten*$^{d/d}$, and *Pten*$^{d/d}$; *Tgfbr1*$^{d/d}$ mice at 2 and 4 weeks of age. Note the increased epithelial hyperplasia at 2 weeks of age (D) and formation of adenocarcinoma foci with necrosis at 4 weeks of age in some *Pten*$^{d/d}$; *Tgfbr1*$^{d/d}$ mice (H) versus *Pten*$^{d/d}$ mice (C, G). A lower magnification was used for E-H versus A-D to capture full images of uterine sections at 4 weeks of age. (I-P) Immunostaining of ER and PGR in the uteri of *Pten*$^{f/f}$, *Pten*$^{f/f}$; *Tgfbr1*$^{f/f}$, *Pten*$^{d/d}$, and *Pten*$^{d/d}$; *Tgfbr1*$^{d/d}$ mice. Signals were developed using NovaRED. Sections were counterstained with hematoxylin. Arrows indicate epithelial components lacking PGR expression (P). Immunohistochemistry was performed using at least 3 independent samples per genotype. Scale bar is representatively depicted in (A) and equals 100 μm (A-D), 250 μm (E-H), and 25 μm (I-P).

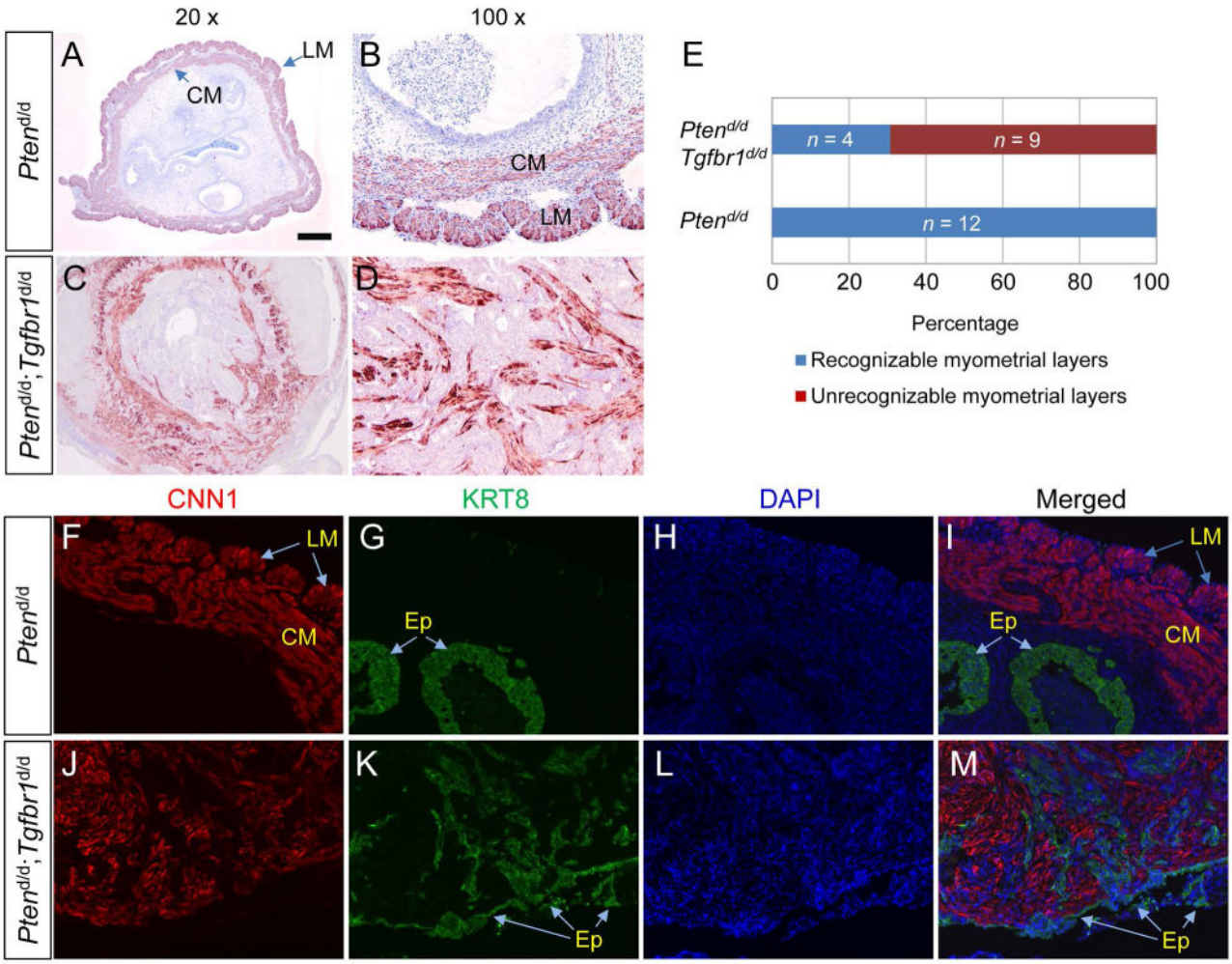

Figure 3.

Myometrial invasion in *Pten*$^{d/d}$; *Tgfbr1*$^{d/d}$ mice. (A-E) Immunohistochemical analysis of myometrial integrity using uteri from *Pten*$^{d/d}$ and *Pten*$^{d/d}$; *Tgfbr1*$^{d/d}$ mice. Representative images of CNN1 staining (9 wk) are shown in panels (A-D) and a summary chart is depicted in panel (E). *Pten*$^{d/d}$ (n = 12) and *Pten*$^{d/d}$; *Tgfbr1*$^{d/d}$ (n = 13) mice at 8 and 9 weeks of age were utilized. (F-M) Double immunofluorescence of KRT8 and CNN1 using uteri of 9-week-old *Pten*$^{d/d}$ and *Pten*$^{d/d}$; *Tgfbr1*$^{d/d}$ mice. Note the severe myometrial invasion/disruption in *Pten*$^{d/d}$; *Tgfbr1*$^{d/d}$ mice compared with *Pten*$^{d/d}$ mice. LM, longitudinal muscle layer; CM, circular muscle layer; Ep, epithelial cells. DAPI was used to counterstain nuclei. Scale bar is representatively depicted in (A) and equals 100 μm (B, D, F-M) and 500 μm (A, C).

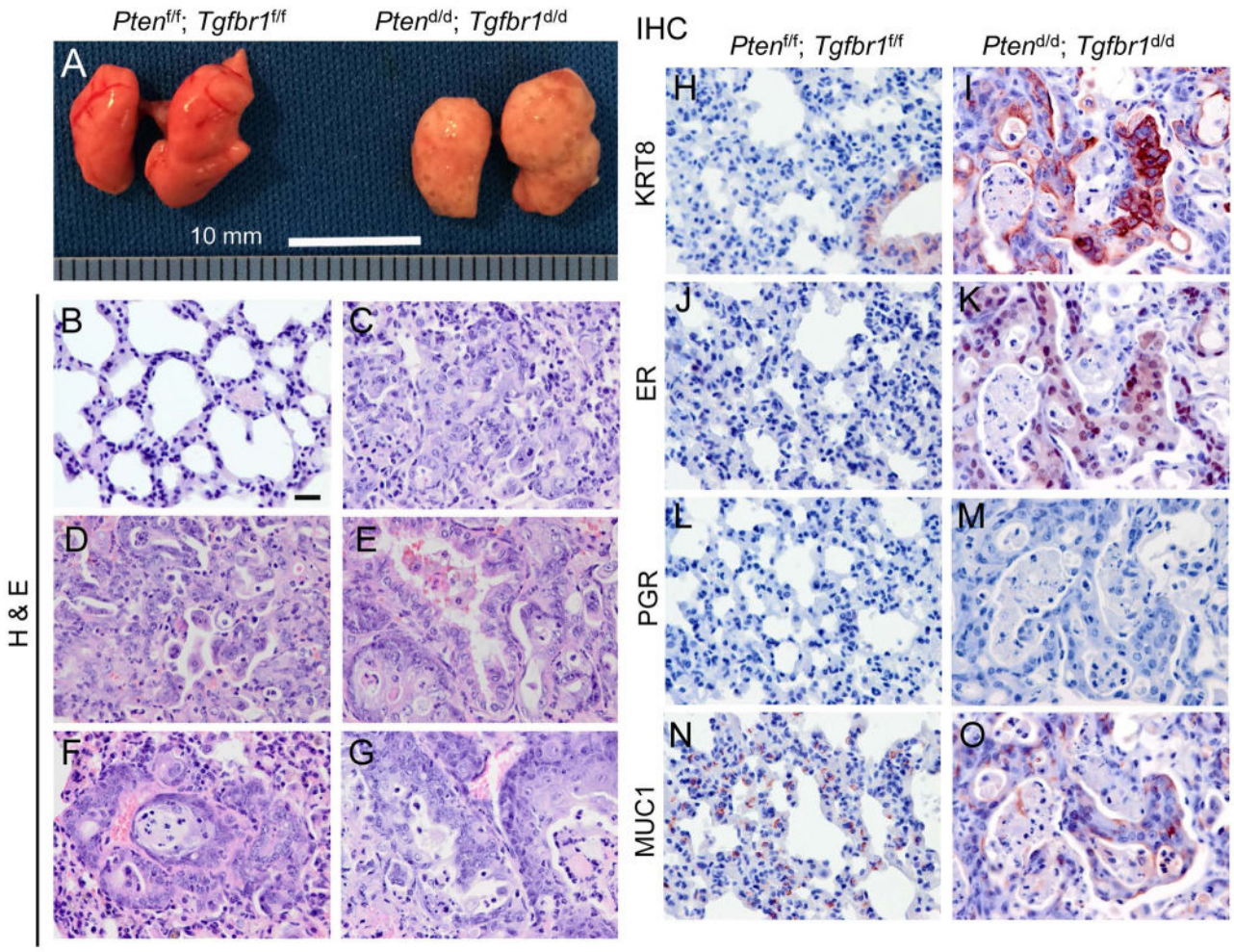

Figure 4.

Conditional deletion of *Pten* and *Tgfbr1* promotes endometrial cancer metastasis. (A) Gross analysis of lung metastases in 7-week-old *Pten*$^{d/d}$; *Tgfbr1*$^{d/d}$ mice versus age-matched *Pten*$^{f/f}$; *Tgfbr1*$^{f/f}$ mice. Note the lungs from *Pten*$^{d/d}$; *Tgfbr1*$^{d/d}$ mice were occupied with tumor foci versus those from *Pten*$^{f/f}$; *Tgfbr1*$^{f/f}$ mice. Scale bar = 10 mm. (B-G) Histological analysis of the lungs from *Pten*$^{d/d}$; *Tgfbr1*$^{d/d}$ and *Pten*$^{f/f}$; *Tgfbr1*$^{f/f}$ mice. Note the presence of highly organized alveoli structures (B) and metastatic nodules containing neoplasms with variable differentiation status (C-G) in the lungs of *Pten*$^{f/f}$; *Tgfbr1*$^{f/f}$ and *Pten*$^{d/d}$; *Tgfbr1*$^{d/d}$ mice, respectively. (H-O) Immunohistochemical staining of lungs from *Pten*$^{f/f}$; *Tgfbr1*$^{f/f}$ and *Pten*$^{d/d}$; *Tgfbr1*$^{d/d}$ mice at 9 weeks of age. Note the metastatic sites were positive for KRT8 (I), ER (K), and MUC1 (O), but not PGR (M). Immunohistochemistry was performed using at least 4 independent lung samples per genotype. Scale bar is representatively depicted in (B) and equals 20 μm (B-O).

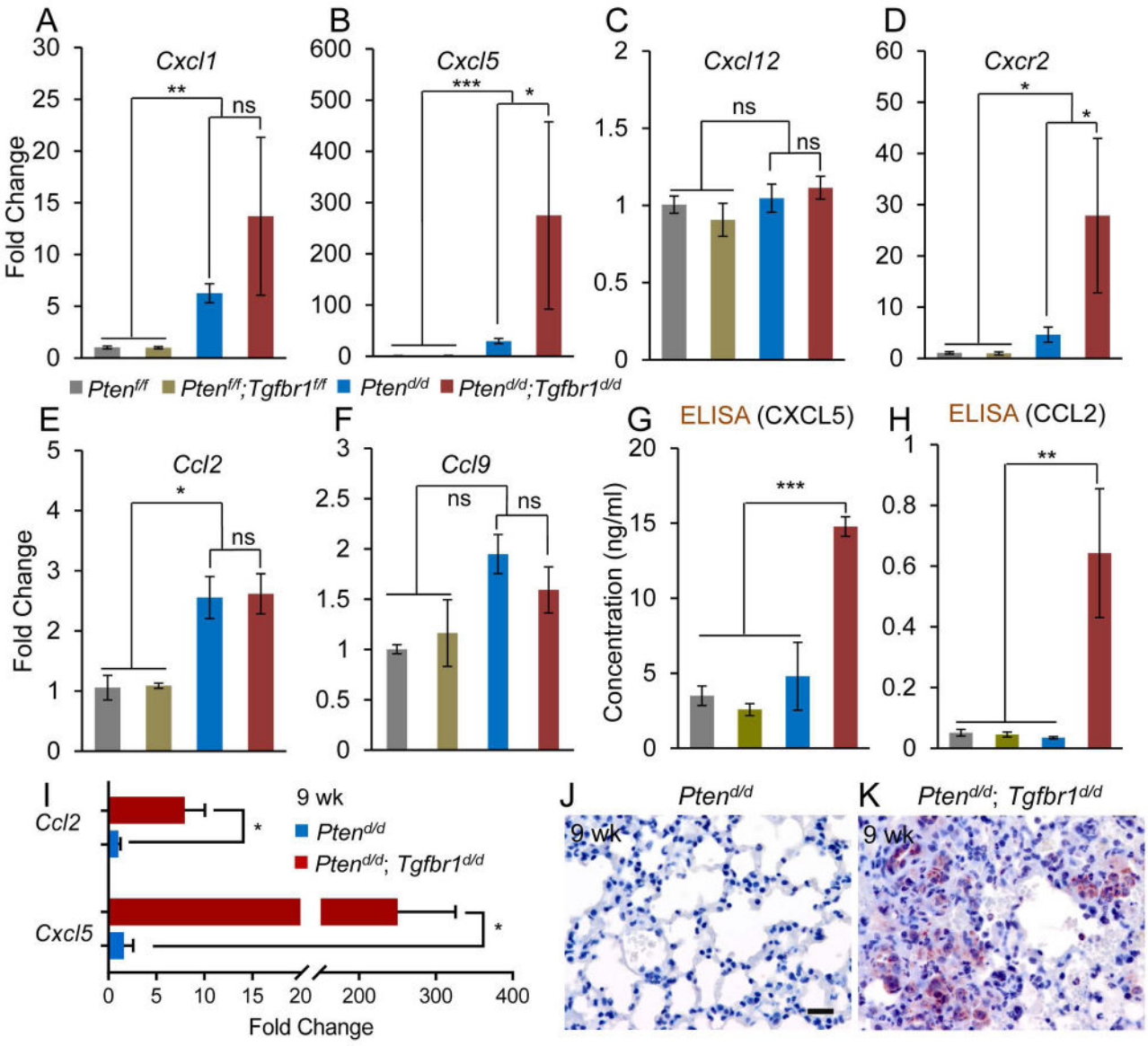

Figure 5.

Alteration of pro-inflammatory chemokine and receptor in *Pten*$^{d/d}$; *Tgfbr1*$^{d/d}$ uteri. (A-F) Expression of select chemokine and receptor in the mouse uterus. Note the expression of *Cxcl5* and *Cxcr2* mRNA was increased in 2-week-old *Pten*$^{d/d}$; *Tgfbr1*$^{d/d}$ mice versus *Pten*$^{d/d}$ and control mice. *Pten*$^{f/f}$ and *Pten*$^{f/f}$; *Tgfbr1*$^{f/f}$ mice were included as normal controls. Real-time PCR was performed using ΔΔCT method. *Rpl19* was used as internal control. $n = 4$-9. (G, H) Serum CXCL5 and CCL2 levels in 9-week-old mice measured by ELISA. $n = 5$. Data are mean ± s.e.m. *$P < 0.05$, **$P < 0.01$, and ***$P < 0.001$. Ns, $P \geq 0.05$. (I) Increased mRNA levels of *Ccl2* and *Cxcl5* in the lungs of *Pten*$^{d/d}$; *Tgfbr1*$^{d/d}$ mice versus *Pten*$^{d/d}$ mice at 9 weeks of age. $n = 4$. Data are mean ± s.e.m. *$P < 0.05$. (J, K) Immunostaining of CXCL5 in the lungs of 9-week-old *Pten*$^{d/d}$ and *Pten*$^{d/d}$; *Tgfbr1*$^{d/d}$ mice. Immunohistochemistry was performed using at least 4 independent lung samples per genotype. Scale bar is representatively shown in (J) and equals 20 μm (J, K).

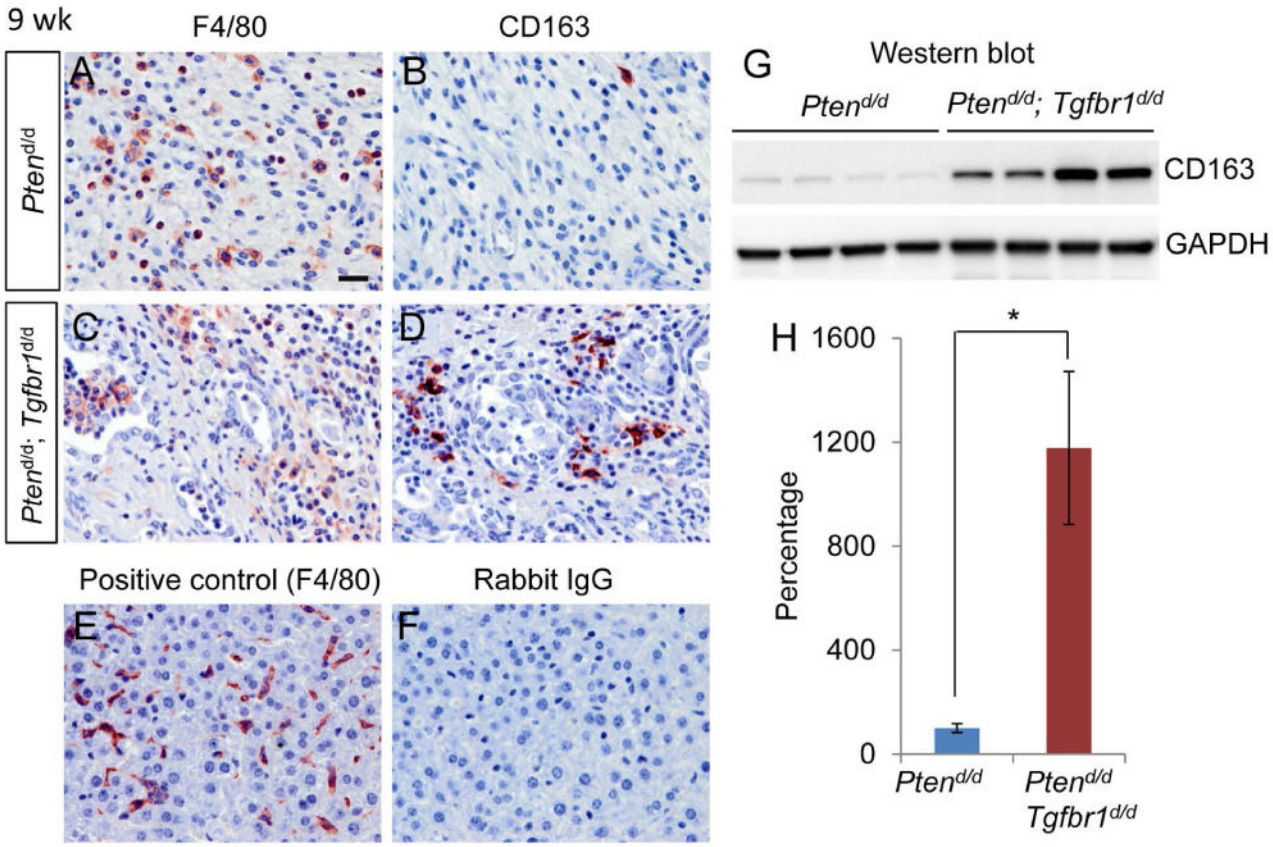

Figure 6.

Expression of F4/80 and CD163 in mice with uterine deletion of *Tgfbr1* and *Pten*. (A-D) Immunostaining of F4/80 and CD163 in the uteri of *Pten*$^{d/d}$ and *Pten*$^{d/d}$; *Tgfbr1*$^{d/d}$ mice at 9 weeks of age. Five independent samples per genotype were examined. (E, F) Representative positive and negative controls for immunohistochemistry. Panel (E) shows a positive control for F4/80 antibody using liver tissues from 9-week-old *Pten*$^{f/f}$ mice, while panel (F) is a negative control using rabbit IgG. Scale bar is representatively depicted in (A) and equals 20 μm (A-F). (G, H) Western blot analysis of CD163 protein expression in the uteri of 9-week-old *Pten*$^{d/d}$ and *Pten*$^{d/d}$; *Tgfbr1*$^{d/d}$ mice. Images for CD163 and GAPDH (internal control) are depicted in panel (G) and quantification result is shown in panel (H). Each lane represents an independent sample. Data are presented as percentage, where CD163 protein levels in *Pten*$^{d/d}$ mice were set to 100%. $n = 4$. Data are mean ± s.e.m. $^{*}P < 0.05$.